Finally, transferring the impedance through the entire network gives a final relationship

$$\frac{Z_n}{Z_0} = \frac{Z_n'}{Z_0'} \tag{34}$$

showing that the networks are identical apart from an overall scaling factor.

References

[1] S. B. Cohn, "Direct-coupled-resonator filters," *Proc. IRE*, vol. 45, pp. 187–196, Feb. 1957.

[2] L. Young, "The quarter-wave transformer prototype circuit," *IRE Trans. Microwave Theory Tech.*, vol. MTT-8, pp. 483–489, Sept. 1960.

[3] ——, "Direct-coupled cavity filters for wide and narrow bandwidths," *IEEE Trans. Microwave Theory Tech.*, vol. MTT-11, pp. 162–178, May 1963.

[4] R. Levy, "Theory of direct-coupled-cavity filters," *IEEE Trans. Microwave Theory Tech.*, vol. MTT-15, pp. 340–348, June 1967.

[5] ——, "A new class of distributed prototype filters with applications to mixed lumped/distributed component design," *IEEE Trans. Microwave Theory Tech.* (*1970 Symposium Issue*), vol. MTT-18, pp. 1064–1071, Dec. 1970.

[6] N. Marcuvitz, Ed., *Waveguide Handbook* (M.I.T. Radiation Laboratory Series), vol. 8. New York: McGraw-Hill, 1951, pp. 120–124.

[7] W. A. Davis and P. J. Khan, "Coaxial bandpass filter design," *IEEE Trans. Microwave Theory Tech.*, vol. MTT-19, pp. 373–380, Apr. 1971.

[8] R. Levy and T. E. Rozzi, "Precise design of coaxial low-pass filters," *IEEE Trans. Microwave Theory Tech.*, vol. MTT-16, pp. 142–147, Mar. 1968.

[9] P. I. Somlo, "The computation of coaxial line step capacitances," *IEEE Trans. Microwave Theory Tech.*, vol. MTT-15, pp. 48–53, Jan. 1967.

[10] H. E. Green, "The numerical solution of some important transmission-line problems," *IEEE Trans. Microwave Theory Tech.*, vol. MTT-13, pp. 676–692, Sept. 1965.

[11] R. Levy, "Synthesis of mixed lumped and distributed impedance-transforming filters," *IEEE Trans. Microwave Theory Tech.*, vol. MTT-20, pp. 223–233, Mar. 1972.

[12] ——, "Tapered corrugated waveguide low-pass filters," this issue, pp. 526–532.

Tapered Corrugated Waveguide Low-Pass Filters

RALPH LEVY

Abstract—**Several new synthesis techniques are described for the design of tapered corrugated waveguide low-pass filters. Previous techniques are based on image-parameter methods which are both nonoptimum and difficult to apply to new specifications. The new synthesis methods give filters which can be constructed to work directly from dimensions generated by a computer. The impedance tapering implies that the terminating impedance transformers used in the image-parameter designs may be either eliminated or reduced in length.**

Introduction

WAVEGUIDE low-pass filters are used in numerous systems, frequently for rejection of spurious harmonics from transmitters. Corrugated waveguide or waffle-iron filters introduced by Cohn [1] are most commonly used for this purpose. The first design methods described in the literature [2] are based on image parameters rather than modern circuit theory, and involve rather complicated procedures requiring empirical adjustments to experimental filters before a satisfactory final design is achieved. Later methods using synthesis techniques have been described very briefly [3] and appear as patents [4], [5]. This paper gives a more complete account of synthesis techniques, including some not reported in the earlier publications.

The major advantages of the synthesis techniques are as follows.

1) The filters may be constructed directly from dimensions printed out by a computer program and work immediately with no major experimental adjustments. In common with other types of waveguide filters, minor tuning adjustments may be required to compensate for mechanical tolerances, especially in small waveguide sizes.

2) The synthesis technique incorporates impedance tapering, so that terminating impedance transformers required in previous designs [2] may be shorter in length, or even completely eliminated. This can result in a length reduction by as much as 3 to 1.

3) The cutoff frequency is predicted exactly, and the VSWR is good in a specified frequency band extending to the cutoff. Hence high attenuation may be specified close to the cutoff frequency f_c, typically 20 dB at $1.05f_c$, or 60 dB at $1.15f_c$.

4) The stopband performance is predicted.

5) Tradeoffs may be made between stop bandwidth, passband insertion loss, and power handling capability.

Several different synthesis techniques have been formulated, but they may be classified in three main categories, as follows.

1) Tapered corrugated capacitive iris filters designed using the distributed low-pass prototype filter [6].

2) Direct realization of a tapered corrugated filter designed using a cascade of unit elements similar to [6], but with a Zolotarev response.

3) A mixed lumped and distributed synthesis using the "half-stub" prototype [7].

The first two methods have been found more generally useful than the third. They are more dissimilar than indicated above, as the detailed description will demonstrate.

A schematic view of the tapered corrugated filter is shown in Fig. 1. The early corrugated filters were periodic structures, but the new designs result in aperiodic structures where the dimensions of the various capacitive and inductive regions

Manuscript received December 6, 1972; revised March 23, 1973.

The author is with Microwave Development Laboratories, Inc., Natick, Mass. 01760.

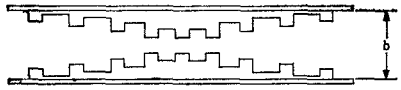

Fig. 1. Tapered corrugated waveguide filter.

vary considerably within the filter. The filter is uniform in the broad dimension, although longitudinal slots could be incorporated as in a waffle-iron filter. The slots complicate the design both theoretically and mechanically, and may be avoided in many applications.

Stopband Characteristics

The insertion loss of a waveguide low-pass filter, assuming H_{10}-mode propagation, is shown in Fig. 2(a). The low-pass filter is actually a bandpass filter in the sense that it will not propagate below a cutoff frequency f_{c_1} (the filter is low pass if plotted with an electrical length or reciprocal guide wavelength abscissa). The cutoff frequency of the filter is f_{01}, and the useful stopband extends from f_{L_1} through f_{U_1}. The harmonic passband above f_{U_1} is located approximately at a frequency where the length of a majority of the inductive cavities become one half of a guide wavelength.

Modes having an electric-field variation in the narrow dimension cannot propagate below a very high cutoff frequency if the narrow dimension is small, and usually only modes of type H_{n0} need to be considered in predicting the location of spurious resonances in the filter. Since the filter is uniform across the broad dimension, the characteristics of the filter may be calculated exactly by locating electric walls at the nodal planes of the electric field, dividing the waveguide into n waveguides in the case of an H_{n0} mode. The performance of the filter in the H_{n0} mode is identical to the performance of one such waveguide of broad dimension a/n, connected to terminating waveguides of the same reduced dimension. Inspection of formulas for the equivalent circuit parameters of a thick capacitive iris shows that these parameters are dependent on the values of λ_g and b, but not on the broad dimension a. Hence the filter will have the same performance in the H_{n0} mode as in the H_{10} mode if both characteristics are plotted on a guide wavelength scale. On a frequency scale, the characteristic of the filter in the H_{n0} mode is shifted upwards in frequency, as indicated in Fig. 2(b). The cutoff frequency of the H_{n0} mode is

$$f_{cn} = nf_{c_1}. \tag{1}$$

The guide wavelength λ_g at free-space wavelength λ_1 for the dominant mode is given by

$$\frac{1}{\lambda_g^2} = \frac{1}{\lambda_1^2} - \frac{1}{\lambda_{c_1}^2} \tag{2}$$

where $\lambda_{c_1} = 2a$ is the cutoff wavelength. In the H_{n0} mode, this guide wavelength is realized at free-space wavelength λ_n given by

$$\frac{1}{\lambda_g^2} = \frac{1}{\lambda_n^2} - \frac{n^2}{\lambda_{c_1}^2}. \tag{3}$$

This leads to the following expression relating a frequency f_1 in the H_{10} mode to a corresponding frequency f_n in the H_{n0} mode, namely

$$f_n = \sqrt{f_1^2 + (n^2 - 1)f_{c_1}^2} \tag{4}$$

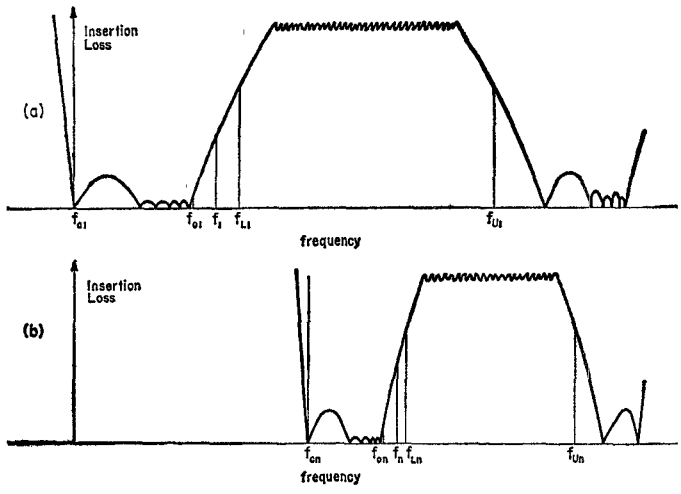

Fig. 2. (a) Insertion loss of filter to the dominant H_{10} mode. (b) Insertion loss to an H_{n0} mode.

TABLE I

Harmonic Bands and Location of Spikes in a WR 137 Filter

n	n^{th} Harmonic band (GHz)	H_{n0}-mode spikes (GHz)
1	5.9 - 6.4	
2	11.8 - 12.8	8.6 - 10.9
3	17.7 - 19.2	12.9 - 14.6
4	23.6 - 25.6	17.2 - 18.5
5		21.5 - 22.5
6		25.8 - 26.7

This formula makes the prediction of the spurious responses in the corrugated filter a relatively simple matter. Spurious responses due to an H_{n0} mode will be located between frequencies f_{cn} and f_n, where f_{cn} is the appropriate cutoff frequency given by (1) and f_n is calculated from (4), f_1 being a frequency above f_{01} where the dominant-mode attenuation is a few decibels. It need not be higher since, in practice, it is difficult to propagate the H_{n0} modes with low attenuation because most of the wave propagation will take place in the dominant mode. The effective attenuation of the filter in regions where H_{n0} modes can propagate is high, and in practice only a few very narrow spurious responses or "spikes" occur which are rarely lower in attenuation than 30 dB. These spikes may be enhanced if the filter is misaligned at the input and output flanges, but are typically 40–50 dB in a well-aligned filter. Spike enhancement also occurs if tuning screws with considerable screw penetration are used.

As an example, consider the design of a filter for the 5.9–6.4 GHz common carrier band in WR 137 (internal dimensions 1.372×0.622 in). The filter is to present high attenuation to the second, third, and fourth harmonics. Assuming that a suitable corrugated filter can be designed and has some attenuation at 8 GHz, then the spikes of low attenuation in the several H_{n0} modes may occur in the frequency bands listed in Table I. It is seen that the second- and fourth-harmonic bands will be completely free of spikes, but a region extending from 17.7 to 18.5 GHz in the third-harmonic band can propagate spikes in the H_{40} mode. In practice, it has been found that the even-ordered modes (H_{20}, H_{40}, etc.) are propagated far less readily than the odd-ordered modes, which is to be expected from symmetry considerations, so that the spikes are likely

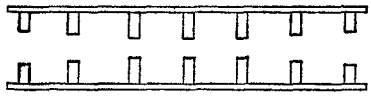

Fig. 3. Capacitive-iris filter.

to be attenuated by 50 dB or more. They may be reduced further by cascading two corrugated filters with spike bands which are interlaced, by introducing a mode filter, by tapering the broad dimension of the filter, or by cutting longitudinal slots in the central uniform region of the filter to form a waffle-iron section. However, as stated, these options complicate the filter and will be unnecessary in most instances.

Synthesis Techniques

Method 1—Tapered Corrugated Capacitive Iris Filters

A very simple type of harmonic rejection filter is a cascade of thick capacitive irises closely spaced in a uniform waveguide, as shown in Fig. 3. The irises are spaced by lengths of waveguide less than $\lambda_g/4$ at cutoff, typically $\lambda_g/8$. The design of this filter is given in [3], [4] and will not be repeated here. It is a special case of a more general class of filters where the waveguide narrow dimension is tapered (in a stepped fashion), as shown in Fig. 1. Since the waveguide narrow dimension is mainly of uniform and full height in Fig. 3, the filter looks like an inductive-iris filter in the H_{01} mode, where the electric field is parallel to the broad dimension of the waveguide. This filter will tend to propagate in this mode at a relatively low frequency usually somewhat lower than three times the primary cutoff frequency of the filter, limiting its use to filters for second- and possibly third-harmonic rejection. It is a very convenient filter for improving the stopband of an inductive-iris bandpass filter, since it may be added with minimal penalty in terms of overall length or cost. An example is given in [3, fig. 2].

The basic design approach for the general tapered corrugated filter is given in [8]. In fact, the waveguide filter may be designed similarly to the coaxial TEM-mode filter [8]. The difference between the two cases lies in the vastly different requirements for the impedance levels in the filter. In the case of the coaxial low-pass filter, the impedances of the internal inductive regions may be, and generally are, much higher than the terminating impedances. In the waveguide case, it is essential that the impedance of the inductive regions be less than that of the terminating impedances, since the waveguide height in the central region of the filter must be small. This imposes certain limitations on the type of prototypes which will result in satisfactory corrugated filters, unless auxiliary impedance transformers are used, as in the image-parameter designs [2].

A simple method of controlling the internal impedance level is by using the generalized distributed low-pass prototype filter [8] shown in Fig. 4. The particular prototype used is a generalization of that described in [6] or in [2, fig. 9.02-1], where the inverter impedances are determined by the values of the junction VSWR's of the ordinary distributed low-pass prototype. In the corrugated filter, each impedance inverter is realized as a thick capacitive iris with short sections of waveguide on each side, as shown in Fig. 5. The various procedures in the design exactly parallel those given in [8] for the design of the coaxial low-pass filter. Hence fringing

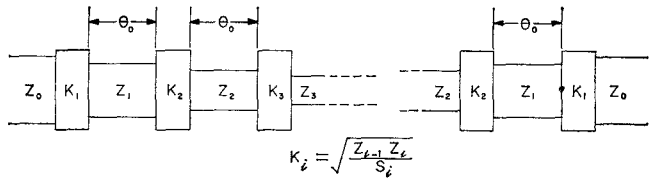

Fig. 4. Generalized distributed low-pass prototype filter.

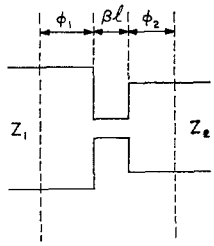

Fig. 5. Impedance inverter formed by a thick capacitive iris.

capacitances and proximity effects are automatically compensated, and the final device should demonstrate good agreement between measured results and the theory.

A typical set of results for a WR 90 filter is shown in Fig. 6. It consists of 11 inductive cavities and is based on a prototype defined by $N=11$, VSWR$=1.02$, and $BW=0.5$ [6]. The length of this filter is 2.435 in, representing a considerable savings in length over a nontapered design which requires impedance transformers at each end.

The theoretical VSWR of the filter in Fig. 6 deviates considerably from the 1.02 VSWR ripple level of the prototype. The deviation is due to the frequency variation of the capacitive impedance inverters. There is also some (smaller) deterioration due to the arbitrary impedance tapering, which should not be too steep for optimum results. There is an infinite number of different designs for a given prototype, obtained by varying the taper and the thickness of the capacitive irises. A few trial designs may be required to obtain the best performance, preferably having large capacitive gaps giving optimum power capability and tolerance sensitivity.

The agreement between theory and practice in Fig. 6 may be improved by the addition of tuning screws. Almost exact agreement between theory and practice is obtainable.

This method gives the shortest low-pass filter having a stopband extending to approximately $3f_c$. A disadvantage is that it is difficult to achieve extremely broad passbands because the VSWR deteriorates at the low end of the band. For example, it is only just possible to design a tapered corrugated filter by this method to pass the 8.2–12.4 GHz standard frequency band for the WR 90 waveguide. However, broader bandwidths for both pass- and stopbands are realizable using the other methods to be described.

Method 2—Direct Unit-Element Realization with Zolotarev Response

This method is an almost direct realization in waveguide of the distributed low-pass prototype filter, for which element values corresponding to Chebyshev equiripple response are given in [6]. However, the Chebyshev response is not optimum unless the VSWR of a low-pass filter is required to be good down to zero frequency, or to the waveguide cutoff fre-

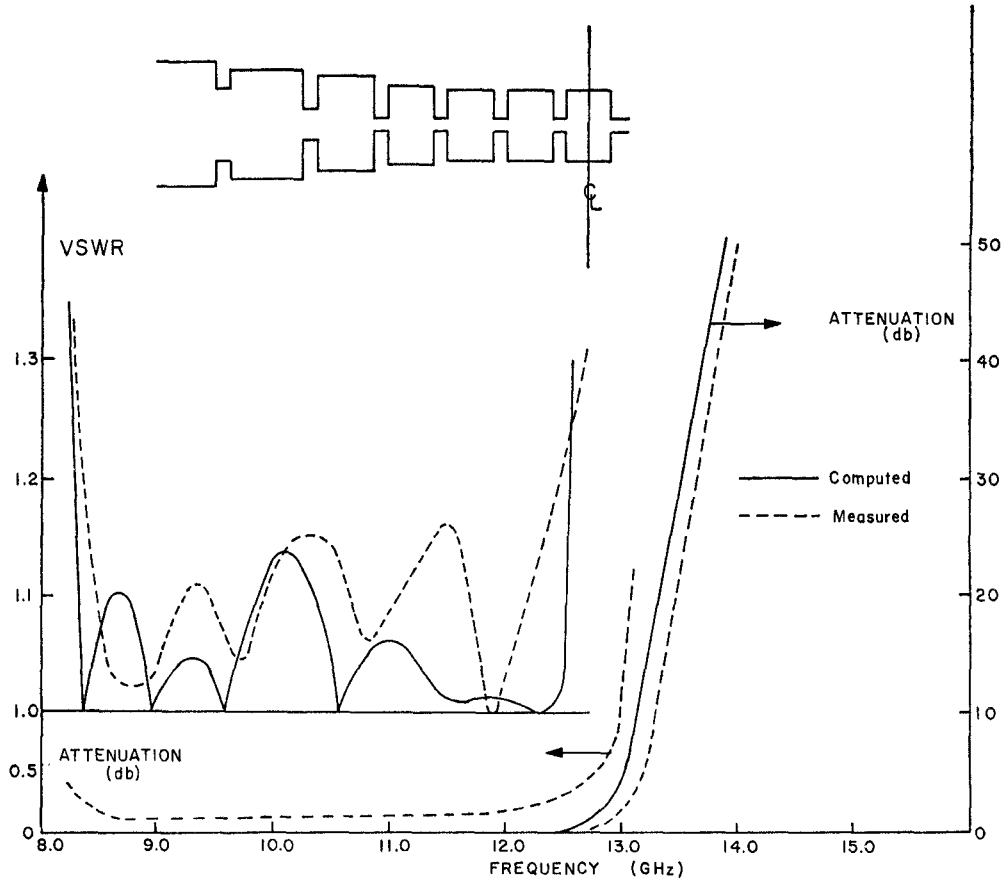

Fig. 6. Eleven-cavity tapered corrugated filter designed by Method 1.

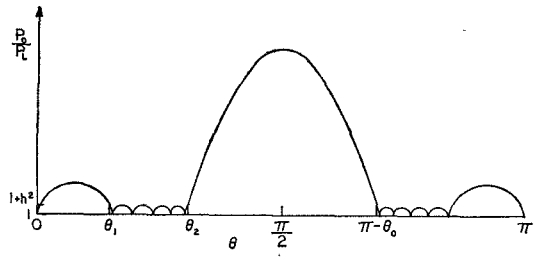

Fig. 7. Insertion loss of distributed low-pass filter with Zolotarev characteristics, used for Method 2.

quency in the case of a waveguide low-pass filter. Obviously, this would rarely be, if ever, a requirement, and in practically every case the Zolotarev (or Achieser–Zolotarev) response [9], [10] would be superior. This filter has an insertion-loss function given by [10]

$$\frac{P_0}{P_L} = 1 + h^2 \operatorname{Zol}_N^2\left(\frac{\sin\theta}{\sin\theta_2}, \lambda\right) \tag{5}$$

where Zol represents a Zolotarev function and

$$\lambda = \frac{\sin\theta_1}{\sin\theta_2} \tag{6}$$

θ_1 defining the lower edge of the equiripple band, as shown in Fig. 7. The Zolotarev function reduces to the Chebyshev function of the first kind when

$$\lambda = \frac{\sin\theta_1}{\sin\theta_2} = \sin\frac{\pi}{2N}. \tag{7}$$

TABLE II

UNIT ELEMENT IMMITTANCES FOR ZOLOTAREV DISTRIBUTED LOW-PASS FILTERS FOR THE CASE $N=2n+1=17$, $\theta_2=21.5°$, VSWR = 1.075

No. \ θ_1	1.938 (Cheb.)	5	6	7	8
1	2.22195	2.42347	2.58493	2.81394	3.09602
2	0.27630	0.28141	0.28901	0.30387	0.32748
3	4.68851	5.06226	5.47622	6.23394	7.51116
4	0.21506	0.23440	0.25913	0.31154	0.41031
5	5.14018	5.77566	6.66985	8.72744	13.3314
6	0.20622	0.23581	0.28041	0.39400	0.67738
7	5.25200	6.12275	7.52152	11.33298	22.2388
8	0.20394	0.23984	0.29941	0.47058	0.99614
9	5.27580	6.23987	7.86229	12.56986	27.5234

Note: See (5)–(7) and Fig. 7 for parameter definitions.

Tables of element values for these Zolotarev distributed filters have not been published, but a sample set of values for the case $N=17$, $\theta_2=21.5°$, and a ripple VSWR of 1.075 is given in Table II. The first column for $\theta_1=1.938°$ corresponds to the unit-element immittances of the Chebyshev case given by condition (7). As θ_1 increases, the immitance values all increase in magnitude, so that if these values are proportional to admittance, the internal admittance level is everywhere higher, i.e., the waveguide heights are everywhere smaller. Alternatively, for a given maximum value of the largest wave-

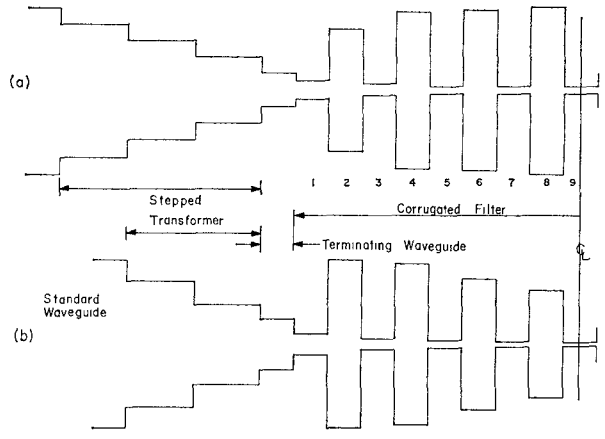

Fig. 8. Comparison between (a) Chebyshev filter and (b) Zolotarev filter with $\theta_1 = 7°$ (heights are to scale, lengths are not).

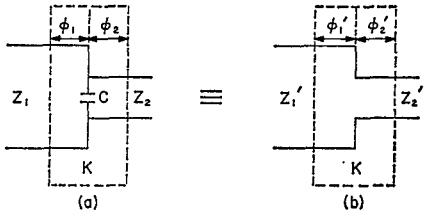

Fig. 9. Equivalence between waveguide E-plane step with (a) junction capacitance and (b) no junction capacitance.

guide height, the terminating waveguide height may be larger, and it will be easier to match the filter to a normal height waveguide. This point is demonstrated in Fig. 8, where the Chebyshev filter whose element values are given in Table II is drawn on the same vertical scale as the Zolotarev filter with $\theta_1 = 7°$, also given in Table II. The two filters are normalized to give maximum waveguide heights which are equal. In the Chebyshev case, this corresponds to one of the central inductive regions, whereas in the Zolotarev case, it corresponds to the first inductive region at each end of the filter. The inductive heights for the two cases are tapered oppositely, i.e., convex for the Chebyshev case and concave for the Zolotarev case. The advantage of the latter is seen to be a terminating waveguide that is larger by a factor of 1.5. Assuming that the largest waveguide height can be made equal to that of the standard waveguide, this means that the impedance transformation required at each end is 5:1 in the Chebyshev case, but only 3.3:1 in the Zolotarev case. As indicated in Fig. 8, this would probably result in a savings of one step in the stepped impedance transformer.

The fringing capacitances in this design are compensated using the generalized impedance-inverter concept [8]. In Method 1, the impedance inverter was taken to be a complete capacitive iris, but here, each step is taken individually, as shown in Fig. 9. The prototype filter has no junction capacitance, and the equivalence between this and the practical filter is made exact at the cutoff frequency by equating the insertion losses (or $K/\sqrt{Z_1 Z_2}$ values) and the location of the impedance-inverter reference planes. At the first junction of the filter we set $Z_1 = Z_1'$ and adjust Z_2 to give the same insertion loss for the junction, i.e., Z_2 is slightly larger than Z_2'. Application of the generalized inverter equations [8] show that $\phi_1 - \phi_1'$ is small and positive, while $\phi_2 - \phi_2'$ has larger numerical value, but is negative. Hence, relative to the prototype filter, the inductive regions are slightly lengthened and the capacitive regions are shortened by a relatively larger

TABLE III
HARMONIC BANDS AND LOCATION OF SPIKES IN AN L-BAND FILTER

n	n^{th} Harmonic band	H_{n_0}-mode spikes (f_1 = 2.15 GHz)	
		a = 4.30 in.	a = 3.80 in.
	(GHz)	(GHz)	(GHz)
1	1.75 - 1.85		
2	3.50 - 3.70	2.74 - 3.20	3.10 - 3.44
3	5.25 - 5.55	4.11 - 4.44	4.66 - 4.89
4	7.00 - 7.40	5.49 - 5.73	6.21 - 6.39
5	8.75 - 9.25	6.86 - 7.06	7.76 - 7.90
6		8.23 - 8.40	9.32 - 9.43
7		9.60 - 9.75	10.87 -10.97

amount. At the second junction we use the new value of Z_2 and adjust Z_3 to give the correct junction insertion loss, and this process is carried out at all junctions of the filter. Proximity effects between nearest junctions across the inductive regions are often significant, and are taken into account as described in [8].

As an example, consider the design of a filter to meet the following specifications:

waveguide	WR 430 (4.30×2.15 in);
passband	1.75–1.85 GHz, VSWR 1.25, insertion loss <0.5 dB;
stopband	>25 dB at 2.2 GHz;
	>70 dB at the second through fifth harmonics of the passband;
	> 40 dB at 10 GHz;
power	5 kW, CW;
length	<24 in.

This specification could be met with a combination of two waffle-iron filters having overlapping stopbands, as described in [2], but the overall length would probably be almost twice that allowed in the specification (the total length occupied by the two 4-step and one 2-step transformers alone would be over 24 in). The Zolotarev design given in Table II ($\theta_1 = 7°$) gives a stopband extending from electrical lengths of 21.5° to 158.5°, a ratio of 7.37:1, and is capable of providing the stopband requirements in a single device. However, it is necessary to ensure that the 70-dB specification is met by avoiding the possibility of any H_{n0}-mode spikes in the specified harmonic bands. Table III gives the location of these spikes both for the WR 430 and for a waveguide of broad dimension equal to 3.80 in, and shows that while a filter built directly in WR 430 would have H_{40}-mode spikes in the third harmonic and H_{50}-mode spikes in the fourth harmonic, reduction of the broad dimension to 3.80 in ensures that the filter will be free of interference in all harmonic bands. The terminating transformers are inhomogeneous rather than homogeneous.

This filter was constructed with a cutoff frequency at 2.1 GHz and has theoretical attenuation of 32 dB at 2.2 GHz, rising to a peak of 220 dB at 6.25 GHz, and drops to 109 dB at 10 GHz and to zero at 10.6 GHz. The computed VSWR in the passband 1.625–2.10 GHz is better than 1.08 compared with 1.075 for the prototype, which demonstrates excellent compensation for the fringing capacitances.

The length of the filter is 7.27 in, and the two 2-step inhomogeneous transformers at each end are each 6.25 in in length. The total length of the filter, including intervening lengths of waveguide, is 22 in. The inhomogeneous transformers were designed on the basis of the general design

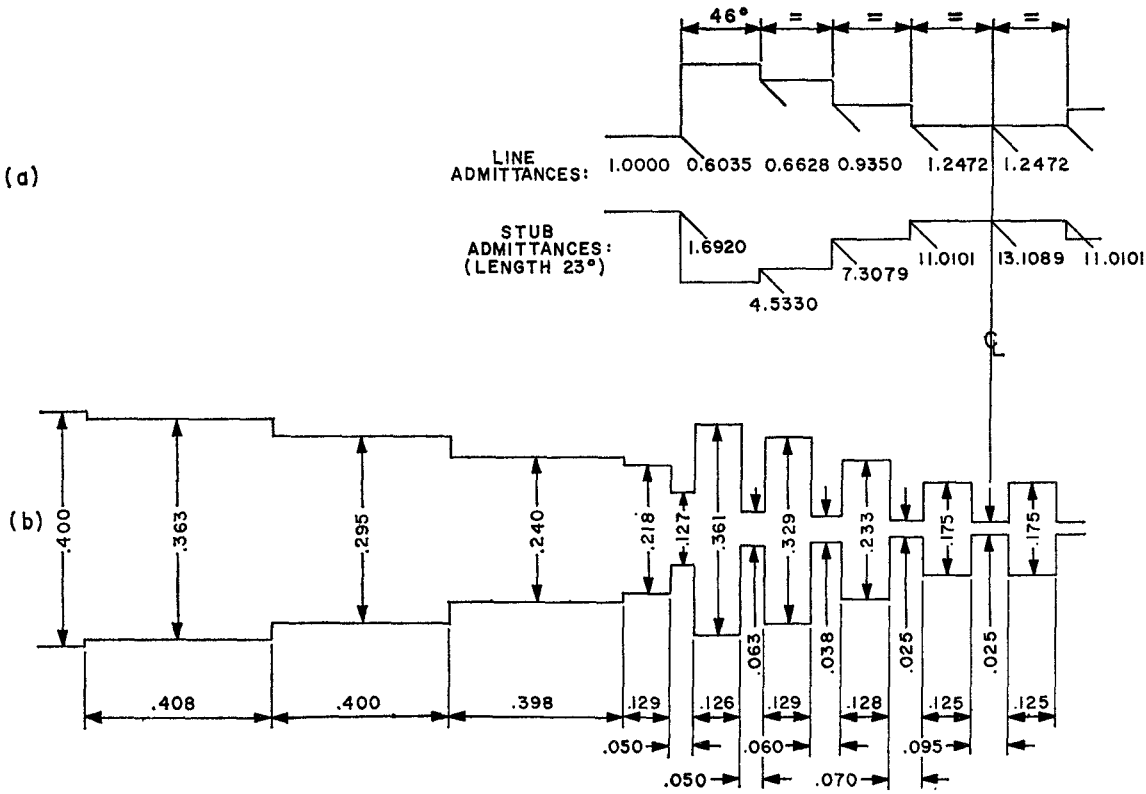

Fig. 10. (a) Zolotarev half-stub prototype used for Method 3. (b) Tapered corrugated filter derived from (a).

philosophy presented in [8] and had a VSWR of less than 1.02 in the 1.75–1.85-GHz band.

The impedance transformers may be reduced in length by about half if the type of mixed lumped and distributed impedance transformer described in [11] is used. This application must be analyzed carefully, however, because this short transformer has a stopband attenuation of its own, and a cascade of two such transformers spaced by a low-pass filter may interact to give large ripples. This is serious only when the first stopband frequency specified is quite close to the passband. In the example considered here, the ripples would not cause problems. Since a program for the design of *inhomogeneous* mixed lumped and distributed transformers had not been completed when this filter was designed, it could not be considered, and the more lengthy conventional transformers were used.

Measurements on the complete filter showed a VSWR of better than 1.07, insertion loss (unplated aluminum) of 0.28 dB, and an H_{10}-mode attenuation in almost exact agreement with theory, measured to a level of 80 dB. The attenuation for all modes in the harmonic bands was greater than 70 dB, as required.

The peak power-handling capability of these filters at normal atmospheric pressure and room temperature may be estimated using the following formula for the breakdown:

$$P = 1.55ab\lambda/\lambda_g \quad \text{(MW)} \tag{8}$$

where a and b are the broad and narrow dimensions in inches of the smallest waveguide section and λ/λ_g is the ratio of free-space to guide wavelengths. In the WR 430 filter described, we have $a = 3.8$, $b = 0.052$, and $\lambda/\lambda_g = 0.67$, giving a breakdown threshold of approximately 0.2 MW.

The CW power-handling capability depends on the available cooling. The insertion loss of 0.28 dB means that 6.5 percent of the incident power of 5 kW, i.e., 325 W, must be dissipated, a fairly low figure for this large filter. A much lower insertion loss is achievable with silver plating.

Method 3—Mixed Lumped and Distributed Prototype

Method 1 gives an acceptable but nonideal passband VSWR because the prototype does not closely correspond to the practical filter. The distributed low-pass prototype filter will not take proper account of the frequency variation of the capacitive irises. The deviation from the prototype is very large at low frequencies, giving VSWR ripples rising to levels of 1.5 or more, and the effect is more severe if the stopband of the filter is required to be very broad. The advantage of Method 1 is the complete elimination of impedance transformers.

Method 2 is almost exact, but some impedance transformation is required. Method 3 is an alternative to Method 2, and gives rather similar results. It is based on the "half-stub" distributed prototype filter introduced in [7]. This gives an almost ideal design for filters consisting of a cascade of lumped shunt capacitors spaced by transmission lines all of equal length, but of differing impedances. A detailed description of the application of this prototype to the design of coaxial low-pass filters is given in [8]. However, as stated previously, it is necessary to taper the internal impedance level to be low at the center of the filter rather than high, as in the coaxial case. This may be achieved partially by using Zolotarev half-stub prototypes [7]. As in Method 2, it is not possible to match the filter to a waveguide of standard height if the maximum height within the filter is restricted to this standard height, but the impedance transformation required is much less than that needed for Chebyshev prototypes or for image-parameter methods.

The design is illustrated in Fig. 10, which gives the dimensions of a filter for WR 90 waveguide designed for a cutoff frequency of 12.8 GHz. The Zolotarev prototype [7] shown

in Fig. 10(a) is for $n=8$, VSWR $=1.02$, $\theta_1=9.5°$, and $\theta_2=23°$. The guide wavelength at 12.8 GHz is 1.074 in, corresponding to θ_2, and at θ_1 this becomes $(23/9.5)\times 1.074=2.6$ in, which occurs at approximately 8.0 GHz. Analysis of the filter shown in Fig. 10(b) shows that the VSWR is less than 1.07 down to 7.8 GHz. Theoretically, the attenuation is greater than 60 dB from 16.0 to 37.0 GHz, and this is the case for the actual filter apart from the H_{n0}-mode spikes. These spikes are quite severe in this filter, since it has only eight cavities. At least eleven cavities should be used for a more acceptable performance.

The process of equating the filter to the prototype is similar to that described for Method 1. The only difference is in the form of the impedance inverter at each junction in the prototype. A corresponding impedance inverter in the filter is a capacitive iris bounded by waveguides of unequal heights, as shown in Fig. 5. The iris thickness is arbitrary, and the gap is chosen to give a required insertion loss as in Method 1.

Further corroboration of the analysis methods used in this paper is presented by Gunston and Blunden [12]. However, they neglect proximity effects, and do not describe any synthesis techniques.

Conclusions

Tapered corrugated waveguide low-pass filters may be designed accurately by a number of different synthesis techniques and will usually perform satisfactorily without requiring empirical adjustments. The impedance tapering has the advantage that impedance transformers are either completely eliminated or reduced in terms of impedance ratio requirements. The methods have almost infinite flexibility, enabling special requirements to be met in an optimal manner.

Longitudinal slots may be cut in the central regions of these filters to improve their performance to higher order H_{n0} modes, as in conventional waffle-iron filters. However, it is suggested that this is not necessary for many applications, especially when the specification requires high attenuation at restricted regions of the stopband (e.g., harmonics of the passband).

The synthesis techniques presented are based on taking predetermined values of the inductive sections and then designing the capacitive sections of the filter (Methods 1 and 3). It is possible also to base the realization on the inductive sections, i.e., to fix the capacitive heights and to design the inductive heights. This dual technique may prove to be advantageous for some applications.

References

[1] S. B. Cohn, "A theoretical and experimental study of a waveguide filter structure," Office Naval Res., Cruft Lab., Harvard Univ., Cambridge, Mass., Rep. 39, Apr. 25, 1948.
[2] G. L. Matthaei, L. Young, and E. M. T. Jones, *Microwave Filters, Impedance Matching Networks, and Coupling Structures*. New York: McGraw-Hill, 1964, pp. 380–409, 937–952.
[3] R. Levy, "Synthesis of high power harmonic rejection waveguide filters," in *IEEE Microwave Theory and Techniques Int. Symp. Dig.*, pp. 286–290, 1969.
[4] ——, "Waveguide filter having sequence of thick capacitive irises," U.S. Patent 3 577 104, May 4, 1971.
[5] ——, "Aperiodic tapered corrugated waveguide filter," U.S. Patent 3 597 710, Aug. 3, 1971.
[6] ——, "Tables of element values for the distributed low-pass prototype filter," *IEEE Trans. Microwave Theory Tech.*, vol. MTT-13, pp. 514–536, Sept. 1965.
[7] ——, "A new class of distributed prototype filters with applications to mixed lumped/distributed component design," *IEEE Trans. Microwave Theory Tech.* (*1970 Symposium Issue*), vol. MTT-18, pp. 1064–1071, Dec. 1970.
[8] ——, "A generalized design technique for practical distributed reciprocal ladder networks," this issue, pp. 519–526.
[9] ——, "Generalized rational function approximation in finite intervals using Zolotarev functions," *IEEE Trans. Microwave Theory Tech.* (*1970 Symposium Issue*), vol. MTT-18, pp. 1052–1064, Dec. 1970.
[10] ——, "Characteristics and element values of equally terminated Achieser–Zolotarev quasi-low-pass filters," *IEEE Trans. Circuit Theory*, vol. CT-18, pp. 538–544, Sept. 1971.
[11] ——, "Synthesis of mixed lumped and distributed impedance-transforming filters," *IEEE Trans. Microwave Theory Tech.*, vol. MTT-20, pp. 223–233, Mar. 1972.
[12] M. A. R. Gunston and D. F. Blunden, "A simplified analysis of corrugated waveguide structures," *Marconi Rev.*, vol. 33, pp. 260–266, 1970.